

Methanol electrooxidation on platinum spontaneously deposited on unsupported and carbon-supported ruthenium nanoparticles

S.T. Kuk, A. Wieckowski*

Department of Chemistry, University of Illinois at Urbana-Champaign, Urbana, IL 61801, USA

Received 29 June 2004; received in revised form 24 August 2004; accepted 24 August 2004

Abstract

Using an inverted spontaneous deposition method, unsupported Ru and carbon-supported 40% Ru nanoparticles were decorated with platinum after surface Ru oxides were reduced in the hydrogen atmosphere at 25 °C for 1 h. All samples that we produced in this way yielded high catalytic activity towards methanol oxidation at an electrode potential of interest to DMFC fuel cells. In the chronoamperometric experiment, the activity increased with the uptake of platinum to high Pt packing density values. The 40% C/Ru/Pt catalyst with an optimized packing density shows higher reactivity than that of an equivalent commercial, carbon-supported Pt/Ru catalyst. Reduction of Ru (and Ru/Pt) nanoparticles at higher than ambient temperature induced unacceptable level of sintering, and was avoided.
© 2004 Elsevier B.V. All rights reserved.

Keywords: Electrocatalysis; Fuel cells; Pt deposition; Ru/Pt nanoparticles; Anode; Methanol

1. Introduction

There is a need for more potent, lightweight, efficient and reliable power-sources for a variety of transportation, portable electronics and other applications [1]. Batteries and fuel cells are alternative energy devices but batteries are only viewed as a short/mid-term option. Fuel cells are efficient energy conversion devices in which both fuel and oxidant are fed in a continuous supply to the electrodes for conversion into electrochemical energy. They have many benefits, including low or even zero emissions, higher efficiency and reliability. The best fuel for fuel cells is pure hydrogen but the use of compressed hydrogen is troubled with inherent problems associated with safety, hydrogen distribution, handling, and storage. Alternative fuels are being sought to replace hydrogen in fuel cells, such as methanol, ethanol and formic acid (and others) with varied success.

Methanol is considered an ideal molecular fuel because of its availability, ease of handling and storage, and is the

basis of the design of a direct methanol fuel cell (DMFC). Methanol has a high energy density, with the full oxidation to CO₂ occurring through a six-electron reaction, and is a promising candidate for energy applications, for instance, in portable electronics. The obstacles against the implementation of DMFC are the insufficient activity of the catalysts employed so far, and high cost of platinum in platinum-based bimetallic catalysts [1–11]. From among such Pt-based bimetallic electrocatalysts, PtRu alloyed or Ru decorated Pt [12] materials are known to be the most active.

Recently, Adzic and coworkers reported Pt-covered Ru(0001) single crystal electrodes of very interesting structure/reactivity properties [13] and Pt decorated Ru nanoparticles [14]. Those were obtained by reduction of ruthenium nanoparticles in H₂ atmosphere at 150–350 °C, and by adding platinum to ruthenium by the use of spontaneous deposition. Notice that the deposition method in the quoted work is an invert of the procedure reported in Refs. [11,15], and may be considered as an “inverted spontaneous deposition”. That is, ruthenium was deposited on platinum nanoparticles in our previous efforts while in this work platinum was deposited on ruthenium nanoparticles, and used for methanol oxida-

* Corresponding author. Tel.: +1 217 333 7943; fax: +1 217 244 8068.
E-mail address: andrzej@scs.uiuc.edu (A. Wieckowski).

tion studies. The quoted authors found high activity of such a Ru/Pt nanoparticle catalyst for reformat oxidation [14]. Low load of platinum in the catalysts was highlighted. Arico et al. [16] investigated high temperature operation of DMFCs based on an unsupported, Ru/Pt catalyst prepared in-house, and reported a DMFC power density of 150 mW cm^{-2} at 130°C under air feed fuel cell operation. At such high temperatures however Ru alone is active to methanol [17], the challenge therefore appears to design the Ru/Pt catalysts operational at lower temperatures (lower than 80°C). Our data refer to this mode of DMFC applications.

The spontaneous deposition of platinum into ruthenium matrices allows excellent utilization of expensive platinum in the Ru/Pt catalyst [13,14]. That is, the deposition of Pt on the Ru nanoparticles leads to improved Ru/Pt electrocatalysts with considerably reduced Pt loading [13,14,16,18,19]. In this study, we have explored the Ru/Pt catalysts (unsupported and carbon supported) for methanol electrooxidation catalysis. The surface composition was examined via inductively coupled plasma (ICP) and through CO stripping voltammetry [20]. Methanol oxidations was monitored using chronoamperometry [20].

2. Experimental

The Ru/Pt catalyst preparation involves the application of a series of pretreatments of Ru and Ru/Pt nanoparticles. Namely, using consecutive reduction of ruthenium oxides by hydrogen (3 h reduction at a given temperature) and spontaneous deposition of Pt on the freshly reduced ruthenium surface (for 1 h). The reduction and deposition processes were repeated four times to generate four Ru/Pt catalysts with increasing amount of platinum (see below). (The first Ru/Pt sample was obtained from Ru black, the second was obtained from the Ru/Pt (1 h) sample, again reduced by hydrogen (3 h) and processed by spontaneous deposition (1 h), to obtain the Ru/Pt (2 h) sample, etc.)

Unsupported and carbon supported nanoparticle Ru samples were reduced in the apparatus shown in Fig. 1. The preheating tubing of this apparatus was used for balancing the inlet gas temperature and the three-way valves were used to change gas (and water) pathways. About 30 mg of an as-received unsupported Ru black (Alfa Aesar, 99.9%, lot # E20N28), Ru/Pt obtained from the Ru (see above), or supported 40% Ru/C commercial catalyst (E-TEK 40% Ru on Vulcan XC-72, lot # 27641199) was placed on the bottom of the flask. The tubing and the flask were immersed in the silicone oil bath and were kept at 100, 160 and 220°C , or thermostated at 25°C , for a predetermined time (0.2–10 h). During the reduction, hydrogen gas was flowing at the rate of $100\text{--}200 \text{ mL min}^{-1}$. When higher than ambient temperature was used, the bath was subsequently cooled down to the room temperature under argon atmosphere to isolate the sample from the ambient upon cooling. Once the room temperature was reached, deoxygenated Millipore water was in-

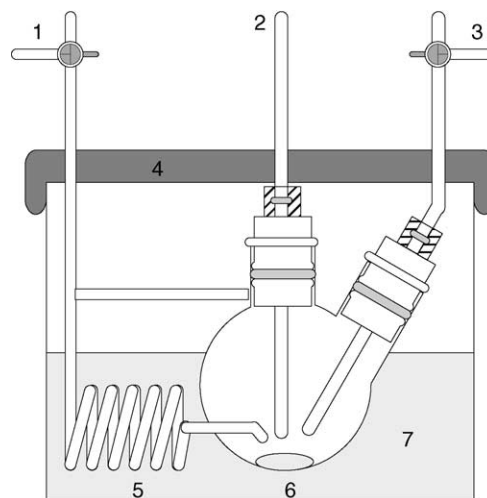


Fig. 1. The apparatus for reduction of Ru samples by hydrogen: (1) three-way stopcock for Ar inlet and H_2 inlet; (2) thermometer; (3) three-way stopcock for gas outlet and H_2O injection; (4) aluminum cover; (5) gas preheating tubing; (6) sample; (7) silicone oil.

jected to the apparatus in order to protect the Ru surface by water and prevent its oxidation. Wet nanoparticle samples thus obtained were transferred to a beaker, and ca. 60 mL (for ca. 30 mg samples) of a 10 mM $\text{K}_2\text{PtCl}_4/0.1 \text{ M H}_2\text{SO}_4$ solution was admitted to the beaker. The suspension of the Ru/Pt nanoparticles was stirred for 1 h in air and the Ru/Pt nanoparticles were isolated after rinsing with 0.1 M H_2SO_4 and Millipore water.

A conventional three-electrode electrochemical cell [21] was used for the electrochemical measurements, with a high surface area Pt gauze as the counter electrode and a Ag/AgCl in 3 M NaCl reference electrode (all potentials in this paper are quoted versus the RHE electrode), powered by an EG&G 283 potentiostat/galvanostat. The working electrode was made of the Ru/Pt catalyst or 40% C/Ru/Pt particles immobilized on a surface of a gold disk (10 mm in diameter, 5 mm in height). A 0.5 M H_2SO_4 was used as the supporting electrolyte, prepared from concentrated analytical grade sulfuric acid from Mallinckrodt Baker diluted in Millipore water. The catalyst was next distributed in Millipore water to make 4 mg mL^{-1} suspension [20]. Approximately $100 \mu\text{L}$ (0.4 mg) of the catalyst ink was loaded on the surface of the Au disk and dried under an IR lamp for 15 min [20]. CO was adsorbed on the surface of the sample catalysts by bubbling CO gas at 1 atm for 20–40 min while holding the potential at 0.06 V. CO was next eliminated from solution by purging the electrolyte with Ar gas for 20–40 min. CO stripping voltammograms were obtained through voltammetric oxidation of CO to measure the active surface area of the catalysts [20].

Unless otherwise stated, chronoamperometric (CA) curves were acquired by stepping the electrode potential to 0.05 V versus RHE in pure supporting electrolyte, holding the electrode until current induced by the step decayed, and then quickly injecting a concentrated methanol solution to a final concentration of 0.5 M methanol under active stirring condi-

tions. This was followed by a potential step to the potential of interest for methanol oxidation and the current was measured usually after 3 h of methanol oxidation. Johnson and Matthey 50:50 PtRu alloy catalyst (HiSPEC™ 6000, 2.5 nm diameter) and E-TEK carbon-supported 40% PtRu alloy (40% PtRu on Vulcan XC-72, 1:1 a/o Pt:Ru, lot # 2239696) Pt were used as standards for the comparison with the methanol oxidation activity of our Ru/Pt decorated catalysts. Ultra high purity argon gas was used to remove the oxygen in the cell. Methanol was ACS grade (Fisher Scientific), and other solutions were made of H₂SO₄ (GFS Chemicals) and K₂PtCl₄ (Alfa Aesar) chemicals. All CO stripping voltammetry tests as well as activity measurements for methanol oxidation were carried out at room temperature.

3. Results and discussion

First, the reduction process was carried out at 220 °C using consecutive hydrogen reduction and spontaneous deposition processes as reported in Section 2. As also stated above, the surface area was calculated from CO stripping methanol oxidation current was measured by chronoamperometry at 0.4 V in 0.5 M methanol in 0.5 M H₂SO₄ [20]. The factor used for converting the CO stripping charge to the surface area is 420 μC cm⁻². The plots shown in Fig. 2 indicate that the methanol oxidation current taken after 3 h of measurements increased with the number of treatments, that is, with the amount of platinum added [20,22]. Concurrently however, the surface area of Ru/Pt catalysts decreased. The obvious

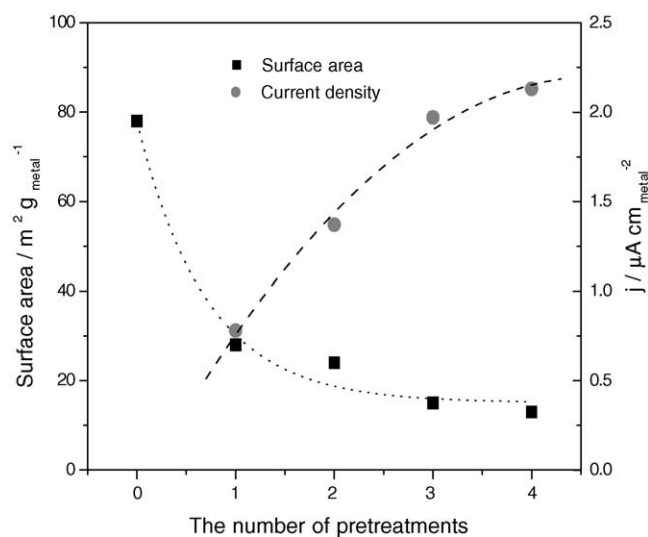


Fig. 2. Changes in the surface area inferred from CO stripping peaks and in the current density at 0.4 V of methanol oxidation on a Pt deposited Ru black (Ru/Pt) catalyst with an increased number of pretreatments. A 0.5 M CH₃OH, in 0.5 M H₂SO₄, at 25 °C. The sample reduction by hydrogen was carried out at 220 °C (in the apparatus shown in Fig. 1). The pretreatment covers two consecutive processes; the reduction at 220 °C for 3 h under hydrogen and the spontaneous deposition of PtRu for 1 h using 10 mM K₂PtCl₄ solution (see text).

Table 1

Current density (in μA cm⁻²) for methanol oxidation at 0.4 V and after 3 h of oxidation obtained using hydrogen reduced unsupported Ru/Pt catalysts (see text)

Reduction time (h)	Reduction temperature (°C)			
	25	100	160	220
0.2	0.69 (78)			
1	1.01 (64)		0.62 (33)	0.60 (33)
2			0.67 (38)	
3				0.61 (28)
4			0.67 (36)	
10	0.93 (66)	0.52 (30)		0.48 (22)
20	0.78 (63)			

Corresponding surface areas (in m² g⁻¹) are listed as the figures in parentheses. The current density and surface areas are shown as function of the reduction time (in the hydrogen gas) and temperature.

reason for the latter effect is sintering of the unsupported Ru particles by the repetition of the heat treatment under H₂ gas atmosphere. Clearly, in order to obtain Ru/Pt catalysts with large specific surface area and high reactivity, the reduction process requires milder conditions than this chosen in Fig. 2.

Table 1 shows the current density for methanol oxidation and the surface area of the unsupported Ru/Pt catalysts obtained after reduction processes under various reduction times and temperature. The data demonstrate that the optimum conditions to get the best Ru/Pt catalyst require the modest reduction temperature of 25 °C (near room temperature), and a time of 1 h. Under such mild conditions, we still managed to maintain the high dispersion of the Ru/Pt catalysts. CO stripping voltammograms of all Ru/Pt catalysts are presented in Fig. 3. (Notice that Fig. 3a shows CVs for pure Pt nanoparticle sample made of Pt black.)

Platinum packing density of Ru/Pt catalysts was calculated by the method reported in a previous communication from this laboratory [20]. Namely, the mass of Pt and Ru ratio from a sample of a known total mass was obtained by using ICP and the Pt packing densities (θ_{Pt}) were calculated from the formula [20]:

$$\theta_{Pt} = \frac{m_{Pt}}{m_{Ru}} \frac{N_A}{S \Gamma_{Ru} M_{Pt}} \quad (1)$$

where m_{Pt} and m_{Ru} are the mass values of platinum and ruthenium, N_A the Avogadro constant, S the specific surface area of the catalyst (cm² g⁻¹), Γ_{Ru} the number of Ru sites cm⁻², and M_{Pt} is the atomic mass of Pt. Γ_{Ru} was taken as 1.63×10^{15} surface atoms cm⁻² (based upon crystallographic data in [23,24]). The electrochemically active surface area of the catalysts was determined from the total amount of adsorbed CO, assuming that the coverage of the saturated CO adlayer is identical on Ru and Ru/Pt surfaces [20].

The packing densities of platinum in the unsupported Ru/Pt catalyst obtained using Eq. (1) for the consecutive pretreatments from the first to the fourth are 0.46, 0.90, 1.37 and 1.83. The values of the packing densities higher than 1 indicate either a multilayer buildup of Pt on the Ru particle surface, or a penetration of platinum into the Ru lattice (Pt and Ru

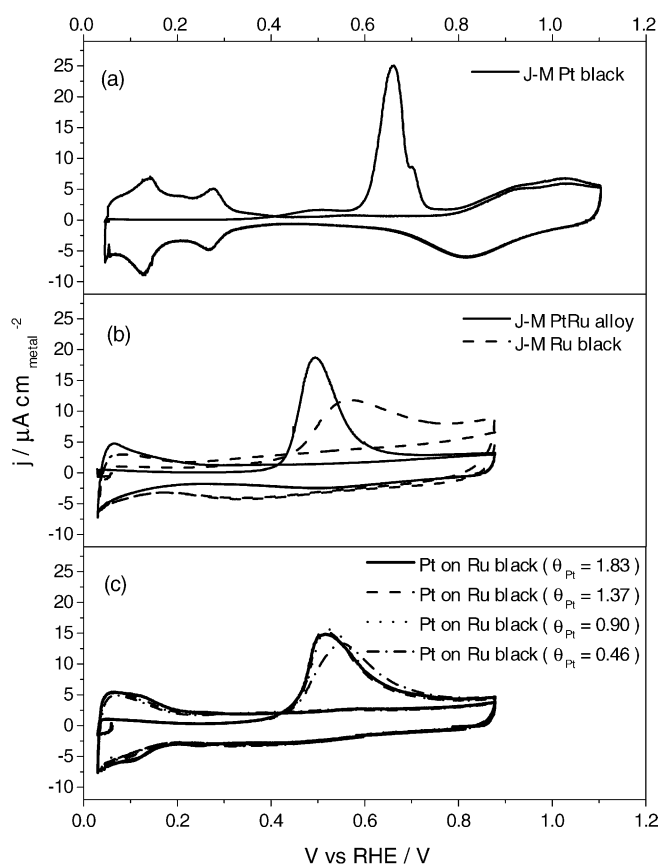


Fig. 3. CO stripping voltammograms on (a) a Pt black electrode, (b) on Johnson and Matthey Pt/Ru alloy and Ru black and (c) on Ru/Pt catalysts of various Pt packing densities. Scan rate 5 mV s^{-1} , $0.5 \text{ M H}_2\text{SO}_4$ supporting electrolyte. The catalyst composition is given.

atoms exchange in the surface zone of the Ru particles) via the cementation process [12]. Some physical properties and CO stripping peak potentials with samples obtained using hydrogen reduction treatment are shown in Table 2. Relevant data on unsupported Ru black or Ru/Pt catalysts and commercial JM PtRu alloy catalyst are also available in this table. The surface area decreases and the CO stripping peak moves to lower potential with the increase in Pt packing density. According to the results of Waszczuk et al. [20], Ru nanosized islands are formed on Ru decorated Pt nanoparticles (using spontaneous deposition). In case of Ru/Pt catalysts, when the Ru phases are activated by hydrogen reduction, the Pt atoms may move into the core of Ru via the cementation process. As it can be seen in Table 2 and Fig. 3c, the CO stripping peaks of Ru/Pt catalyst shift to lower potential with increasing the Pt packing

density but the potential difference is very small ($\sim 34 \text{ mV}$). Similar to the Ru deposited Pt catalysts, Ru/Pt catalysts have high activity for methanol oxidation due to the bifunctional mechanism between the Pt and Ru. (As well-known, the role of Ru in this bifunctional mechanism is to dissociate water to create an oxygen species that converts chemisorbed CO on neighboring Pt atoms to CO_2 [25].) Much excess of platinum of the Ru surface can be eliminated by inspection of the cyclic voltammetric curves in Figs. 3 and 5 that are still much more Ru- than Pt-like. Therefore, the data tend to point at the Pt penetration process, but this issue needs to be investigated further.

Fig. 4 shows chronoamperometric curves for methanol oxidation on Ru/Pt catalysts of various packing densities obtained after the reduction process at 25°C for 1 h. The data indicate that the Ru/Pt catalysts have high activity for methanol oxidation (as a pure Ru sample yields zero or very low current from the oxidation). Clearly, the reactivity is increased with the increase in the Pt uptake; the highest packing density obtained in this study yields the best reactivity. Although the actual Pt:Ru ratio on the outmost (two-dimensional) part of the surface is unknown (see above), one may expect that this ratio is high for platinum. Formally, this would give support to previous results obtained by Gasteiger et al. [25] and Frelink et al. [26] calling for highly Pt enriched Pt/Ru surfaces of polycrystalline PtRu alloys for effective methanol oxidation catalysis. However, the overall Ru/Pt particle morphology that we produce in this report is very much different from that of polycrystalline Pt/Ru used by the other groups [25,26], and care needs to be taken to compare all these results directly. Nevertheless, we conclude that much Pt must be added to the surface zone of the Ru particles in order to obtain high activity, which we believe is a new observation in the methanol fuel cell catalysis field. Still, the high amount of Pt is needed only locally, leaving the overall bulk nanoparticle made of ruthenium. In Table 2, the atomic ratio of commercial JM PtRu alloy catalyst was 1:1 but in case of Pt deposited Ru catalysts, the ratio was 1:7 to 1:12. These values were obtained from the compositions of bulk Ru/Pt nanoparticles and they were different from that of the surface. Therefore, this report demonstrates that relatively low Pt load and high activity Ru/Pt nanoparticle catalyst was obtained by the inverted deposition method [12,15], the result that may have practical implications in the DMFC field. Noticeably however, the catalytic activity of even the highest Pt load is lower than that obtained by the unsupported JM, 50:50 Pt/Ru alloy catalysts, as shown in Fig. 4.

Table 2

Physical properties and CO stripping peak potentials of five different samples obtained using hydrogen reduced, unsupported Ru/Pt catalysts

Sample	Packing density	Pt/Ru (wt.%)	Pt/Ru (atm)	Surface area ($\text{m}^2 \text{g}^{-1}$)	CO stripping peak potential (V)
JM PtRu	–	65.9/34.1	1/1	78	0.492
Ru/Pt-046	0.46	13.4/86.6	1/12	64	0.550
Ru/Pt-090	0.90	17.3/82.7	1/9	44	0.526
Ru/Pt-137	1.37	20.2/79.8	1/8	35	0.514
Ru/Pt-183	1.83	22.5/77.5	1/7	30	0.514

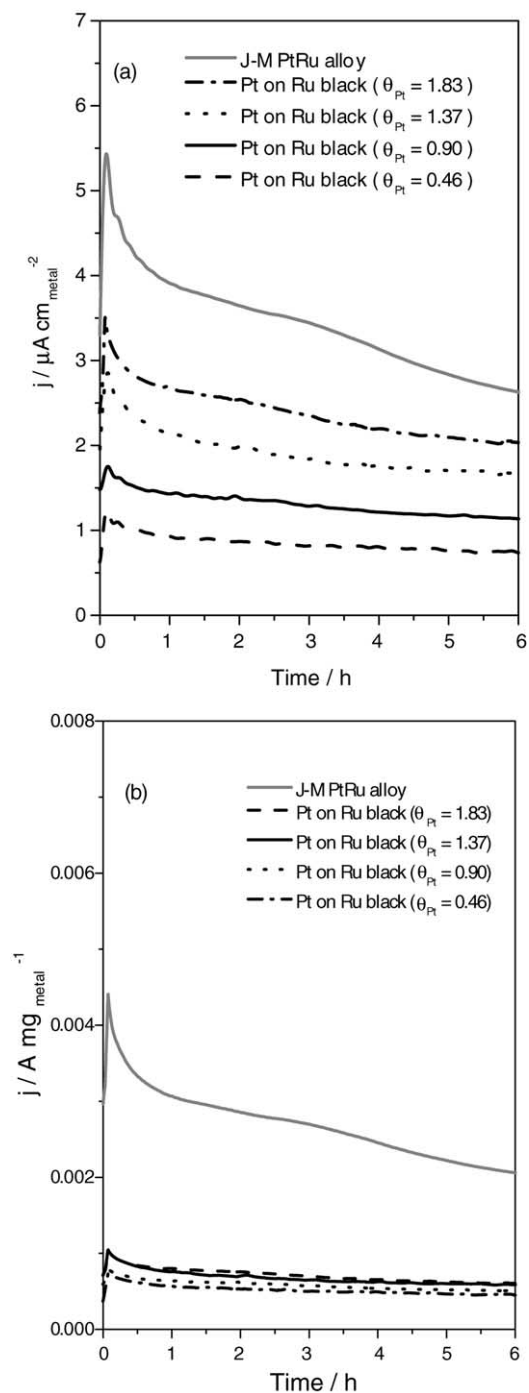


Fig. 4. Chronoamperometric oxidation at 25 °C of methanol at 0.4 V on Pt deposited Ru black (Ru/Pt) catalysts of various Pt packing density (a) for surface area and (b) for unit metal mass. A 0.5 M CH_3OH , in 0.5 M H_2SO_4 . The catalyst composition is given.

Carbon supported catalysts exhibit higher specific activity when compared to the unsupported catalysts (such as reported above) because smaller and spatially separate nanoparticles can be made stable during a catalytic reaction, that is, without meaningful sintering for a long time. In this project we produced a 40% C/Ru/Pt catalyst using 40% C-supported Ru nanoparticles and the Pt spontaneous deposition method

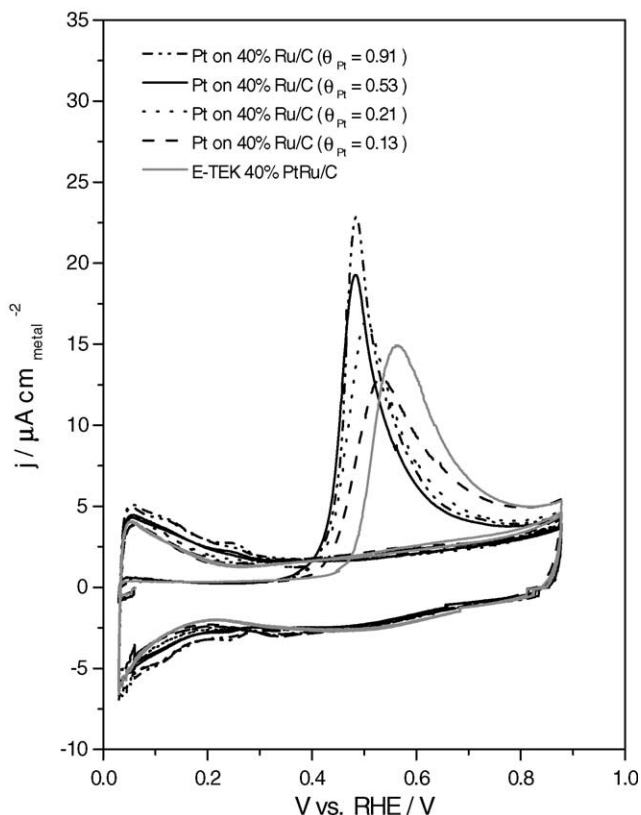


Fig. 5. CO stripping voltammograms on the Ru/Pt catalyst, scan rate 5 mV s^{-1} , 0.5 M H_2SO_4 supporting electrolyte. The catalyst composition is given.

described above. During the deposition, platinum was selectively deposited on Ru particles, not on the carbon support, because only the metallic Ru surface acts as a nucleating agent for the Pt deposition [18]. Table 3 shows essential physical properties and the CO stripping peak potentials of samples obtained after hydrogen reduction for supported Ru/C, C/Ru/Pt, and commercial E-TEK 40% Pt/Ru/C catalysts. The surface area decreases and the CO stripping peak moves to the lower potential with the increase in the packing density similarly to the results with the unsupported samples.

Cyclic voltammetric curves (CVs) for CO electrooxidation on several 40% C/Ru/Pt catalysts – displaying the increased amount of platinum – are given in Fig. 5. The data were obtained at a scan rate of 5 mV s^{-1} in 0.5 M H_2SO_4 . Comparing the data in Fig. 5 to the base CV for pure platinum in Fig. 3a indicates that the surfaces are essentially Ru-like, confirming that the Pt and Ru atoms most likely exchange during the deposition/cementation process, as proposed above for the unsupported sample. The alternative is a strong electronic effect that the Ru matrix may exert on the Pt additives, but this has to be confirmed by a method sensitive to the Ru/Pt electron density of states (DOS) [27] in the studied Ru/Pt atomic configurations.

The peak potential for the CO oxidation shifts negatively as the Pt packing density is increased. However, this potential shift continues only until to the Pt packing density 0.53

Table 3

Physical properties and CO stripping peak potentials of five different samples obtained using hydrogen reduced, carbon-supported C/Ru/Pt catalysts

Sample	Packing density	Pt/Ru/C (wt.%)	Pt/Ru (atm)	Surface area ($\text{m}^2 \text{g}^{-1}$)	CO stripping peak potential (V)
E-TEK PtRu/C	–	26.4/13.6/60.0	1/1	69	0.562
C/Ru/Pt-013	0.13	1.3/39.5/59.2	1/59	51	0.531
C/Ru/Pt-021	0.21	2.2/39.1/58.7	1/34	50	0.504
C/Ru/Pt-053	0.53	4.7/38.1/57.2	1/16	44	0.483
C/Ru/Pt-091	0.91	6.2/37.5/56.3	1/12	34	0.483

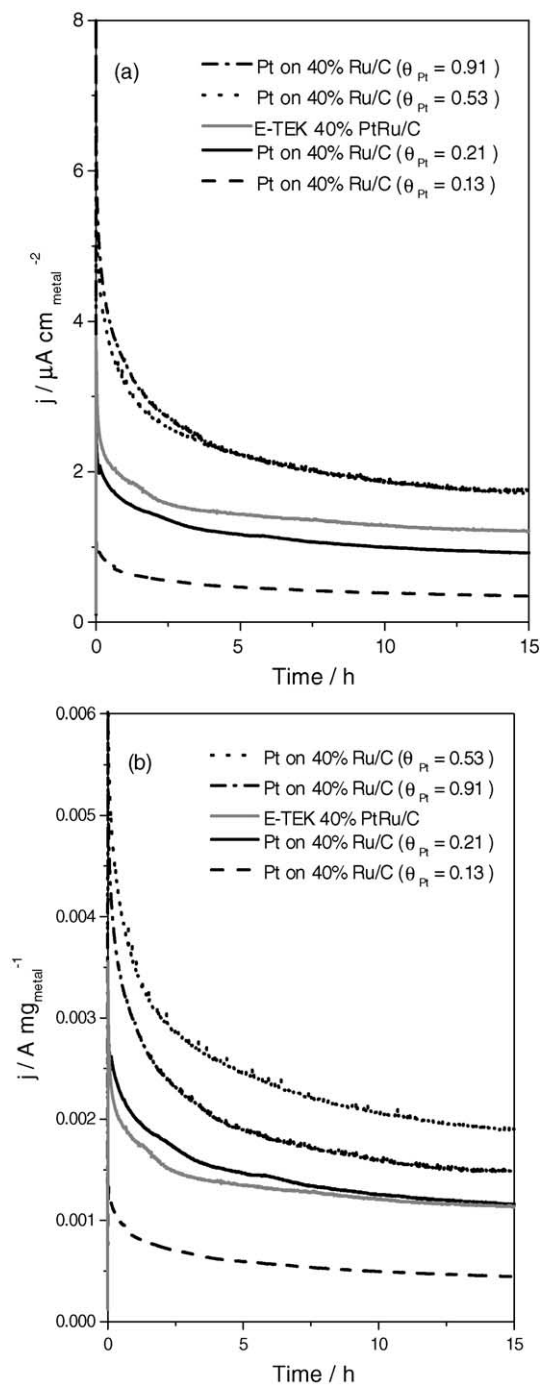


Fig. 6. Methanol oxidation at 25 °C on Pt deposited on 40% Ru/C (40% C/Ru/Pt) catalysts of various Pt packing density (a) for surface area and (b) for unit metal mass. A 0.5 M methanol oxidation at 0.4 V in 0.5 M H_2SO_4 .

is reached (Eq. (1)) was again used for the Pt packing density determination). As above, the meaning of this observation is unclear as the actual composition of the outmost Ru/Pt surface is unknown, but it may show that the 0.53 packing density (or coverage) corresponds to the surface composition of the maximum activity of the catalyst. (Notice that it was reported in [20] that the surface composition of the Pt/Ru catalyst of ca. 0.5 yielded the highest methanol oxidation activity at the same potential.) Chronoamperometric data for methanol oxidation on the supported samples are shown in Fig. 6. Clearly, the 40% C/Ru/Pt catalyst with a packing density of 0.53 displays the highest reactivity, and this value is higher than that of the commercial carbon-supported 40% Ru/Pt catalyst of the 50:50 Ru:Pt ratio (see the central solid-grayish line in Fig. 6). Notably, Gasteiger et al. [25] carried out potentiostatic oxidation of methanol from 0.5 M H_2SO_4 at 25 °C on PtRu alloy electrodes at several Pt/Ru ratios at 0.4 V. Using these quoted results as a benchmark, the reactivities (current densities) of the unsupported and carbon supported Ru catalysts are ca. 30% of the data with the PtRu alloy. Apparently, the higher activity of bulk metal/alloy versus nanoparticle catalysts is still a not completely understood issue.

Overall, while certain saving of platinum could be achieved by our method at the expense of less expensive ruthenium versus commercial Pt/Ru catalysts, the load of platinum is still too high. However, we believe that the reported catalyst syntheses open a possibility to develop a process that can be called “ruthenium matrix catalysis” in which more admetals than platinum will be added to ruthenium nanoparticles. In principle, higher catalytic activity can then be obtained via electronic factors as described in Ref. [28]. This multicomponent preparative path will have yet to be pursued.

4. Conclusions

Unsupported Ru/Pt and carbon-supported C/Ru/Pt nanoparticle catalysts were obtained using inverted spontaneous deposition of platinum to ruthenium following the ruthenium reduction process under hydrogen atmosphere at room temperature. Apparently, a certain level of reduction of Ru oxides occurs under such mild reduction conditions to permit the deposition of platinum into the ruthenium substrate. A part of the deposition most likely occurs via cementation, in which the Pt atoms exchange with the Ru matrix atoms, and penetrate below the two-dimensional Ru/Pt surface towards

the core of the Ru particle. Overall, the activity of all catalysts towards methanol oxidation increases with the increase in the platinum uptake, as shown both in the voltammetric and chronoamperometric experiment. The most promising data were obtained with the 40% C/Ru/Pt catalysts. Here, the 40% C/Ru/Pt catalyst with a packing density of 0.53 has the best reactivity, and this value is higher than that of the commercial carbon-supported 40% Pt/Ru catalyst of the 50:50 Pt:Ru ratio.

These laboratory results need to be tested on the DMFC membrane to indicate possible commercial value of this catalyst synthesis with the catalytic materials reported in this paper.

Acknowledgments

Dr. Hideto Imai's (the NEC Corporation, Japan) contribution is appreciated, and discussions of this project with Dr. R. Adzic of BNL and J. Spindelov of UIUC are gratefully acknowledged. This work was supported by the U.S. Department of Energy, Division of Materials Sciences under Award No. DEFG02-91ER45439, through the Frederick Seitz Materials Research Laboratory at the University of Illinois at Urbana-Champaign and by the National Science Foundation under grant NSF CHE03-4999. STK acknowledges support by the Post-doctoral Fellowship Program of Korea Science and Engineering Foundation (KOSEF) for his first year of work at UIUC.

References

- [1] A. Lamm, H. Gasteiger, W. Vielstich (Eds.), *Handbook of Fuel Cells*, Wiley-VCH, Chester, UK, 2003.
- [2] A. Wieckowski, E. Savinova, C. Vayenas, *Catalysis and Electrocatalysis at Nanoparticle Surfaces*, Marcel Dekker, New York, 2003.
- [3] R. Parsons, T. VanderNoot, *J. Electroanal. Chem.* 257 (1988) 257.
- [4] B. Beden, J.M. Leger, C. Lamy, *Modern Aspects of Electrochemistry*, Plenum Press, New York, 1992.
- [5] H.A. Gasteiger, N. Markovic, P.N. Ross, E.J. Cairns, *J. Phys. Chem.* 97 (1993) 12020.
- [6] M.P. Hogarth, G.A. Hards, *Platinum Met. Rev.* (1996).
- [7] L. Kevin, R.X. Liu, C. Pu, Q. Fan, N. Leyarowska, C. Seger, E.S. Smotkin, *J. Electrochem. Soc.* 144 (1997) 1917.
- [8] B.N. Grgur, N.M. Markovic, P.N. Ross, *J. Electrochim. Acta* 43 (1998) 3631.
- [9] E. Reddington, A. Spienza, B. Gurau, R. Viswanathan, S. Saragapani, E.S. Smotkin, T.E. Mallouk, *Science* 282 (1998) 1735.
- [10] B. Grgur, N. Markovic, P. Ross, *J. Phys. Chem. B* 101 (1998) 3910.
- [11] W. Chrzanowski, A. Wieckowski, *Langmuir* 14 (1998) 1967.
- [12] J.S. Spindelov, A. Wieckowski, Noble metal decoration of single crystal platinum surfaces to create well-defined bimetallic electrocatalysts, PCCP, in press.
- [13] S.R. Brankovic, J.X. Wang, R.R. Adzic, *Electrochem. Solid State Lett.* 4 (2001) A217–A220.
- [14] S.R. Brankovic, J. McBreen, R.R. Adzic, *J. Electroanal. Chem.* 503 (2001) 99.
- [15] W. Chrzanowski, A. Wieckowski, *Langmuir* 13 (1997) 5974.
- [16] A.S. Arico, V. Baglio, E. Modica, A.D. Blasi, V. Antonucci, *Electrochem. Commun.* 6 (2004) 164–169.
- [17] G. Vijayaraghavan, L. Gao, C. Korzeniewski, Methanol electrochemistry at carbon-supported Pt and PtRu fuel cell catalysts: voltammetric and in situ infrared spectroscopic measurements at 23 and 60 °C, *Langmuir* 19 (2003) 2333–2337.
- [18] J.M. Wang, S.R. Brankovic, Y. Zhu, J.C. Hanson, R.R. Adzic, *J. Electrochem. Soc.* 150 (2003) A1108–A1117.
- [19] P. Waszczuk, A. Crown, S. Mitrovski, A. Wieckowski, Methanol and formic acid oxidation on Ad-metal modified electrodes, in: A. Lamm, H. Gasteiger, W. Vielstich (Eds.), *Handbook for Fuel Cells: Fuel Cell Electrocatalysis*, Wiley-VCH, Chester, UK, 2003.
- [20] P. Waszczuk, J. Solla-Gullon, H.S. Kim, Y.Y. Tong, V. Montiel, A. Aldaz, A. Wieckowski, Methanol electrooxidation on platinum/ruthenium nanoparticle catalysts, *J. Catal.* 203 (2001) 1–6.
- [21] G. Tremiliosi-Filho, H. Kim, W. Chrzanowski, A. Wieckowski, B. Grzybowska, P. Kulesza, *J. Electroanal. Chem.* 467 (1999) 143–156.
- [22] A. Crown, C. Johnston, A. Wieckowski, *Surf. Sci.* 506 (2002) L268–L274.
- [23] J.R. Anderson, *Structure of Metallic Catalysts*, Academic Press, 1975.
- [24] C. Bracchini, V. Indovina, S. Rossi, L. Giorgi, *Catal. Today* 55 (2000) 45–49.
- [25] H.A. Gasteiger, N. Markovic, P.N. Ross, E.J. Cairns, *J. Electrochem. Soc.* 141 (1994) 1795.
- [26] T. Frelink, W. Visscher, J.A.R.V. Veen, *Langmuir* 12 (1996) 3702–3708.
- [27] P.K. Babu, E. Oldfield, A. Wieckowski, Nanoparticle surfaces studied by electrochemical NMR, in: R.E. White (Ed.), *Modern Aspects of Electrochemistry*, Kluwer Academic Publishers/Plenum Press, New York, NY, 2003.
- [28] Y.Y. Tong, H.S. Kim, P.K. Babu, P. Waszczuk, A. Wieckowski, E. Oldfield, *J. Am. Chem. Soc.* 124 (2002) 468.